Iraqi Journal of Physics, 2021 *Vol.19, No.49, PP. 22-31*

DOI: 10.30723/ijp.19.49.22-31

Structural and Optical Properties of Tio_2:Nio Nanoparticles Thin Films Prepare by Chemical Spray Pyrolysis

Wasan A. Al-Taa'y[1], Bushra A. Hasan[2]

[1]Department of Physics, College of Science, AL-Nahrain University, Baghdad, Iraq

[2]Department of Physics, College of Science, Baghdad University, Baghdad, Iraq

E-mail: bushra_abhasan@yahoo.com

Corresponding author: wasanali100@yahoo.com

Abstract

The structural and optical properties of pure and doped nano titanium dioxide (TiO_2) films, prepared using chemical spray pyrolysis (CSP) technique, with different nano-size nickel oxide (NiO) concentrations in the range (3-9) wt% have been studied. X-Ray diffraction (XRD) technique was used to analysis the structure of the prepared thin films. The results revealed that the structure properties of TiO_2 was polycrystalline with anatase phase. The parameters, energy gap, extinction coefficient, refractive index and real and imaginary parts were studied using absorbance and transmittance measurements from a computerized ultraviolet visible spectrophotometer in the wavelengths range (300-800) nm. Optical properties of TiO_2 were affected by the addition of NiO impurity where the transmittance increased as NiO concentration increased but with more adding the transmittance returned to decrease again. It was found that the extinction coefficient, refractive index and real and imaginary parts values decreased with increasing the doping percentage up to 7% and then increases again at 9%. Energy gap values increased after doping with NiO where the values were in the range was 3.31 to 3.51 eV.

Key words

TiO_2 metal oxide, NiO nickle oxide, structure and Optical properties.

Article info.

Received: Oct. 2020

Accepted: Feb. 2021

Published: Jun. 2021

الخصائص التركيبية والبصرية للاغشية الرقيقة النانوية TiO_2:NiO المحضرة بواسطة الرش الكيميائي الحراري

وسن علي الطائي[1]، بشرى عباس حسن[2]

[1]قسم الفيزياء، كلية العلوم، جامعة النهرين، بغداد، العراق

[2]قسم الفيزياء، كلية العلوم، جامعة بغداد، بغداد، العراق

الخلاصة

تمت دراسة الخصائص التركيبية والبصرية لاغشية اوكسيد التيتانيوم TiO_2 النقي والمشوب المحضرة باستعمال تقنية الرش الكيميائي الحراري، مع دراسة اضافة نسب مختلفة من اوكسيد النيكل النانوي NiO بمدى تركيز wt% (3-9). استخدمت تقنية حيود الاشعة السينية لتحليل الخواص التركيبية للاغشية المحضرة. النتائج توصلت الى ان غشاء TiO_2 يمتلك تركيب متعدد التبلور بطور الانتاس. درست المعلمات فجوة الطاقة معامل الخمود، معامل الانكسار، الاجزاء الحقيقي والخيالي درست باستخدام قياسات الامتصاصية والانبعاثية من جهاز المطياف بمدى اطوال موجية (300-800) nm. تاثرت الخواص البصرية ل TiO_2 نتيجة اضافة الشائبة NiO حيث زادت الانبعاثية مع زيادة التركيز لكنها انخفضت مع النسب العالية للتشويب. وجد ان قيم معامل الخمود، معامل الانكسار، الاجزاء الحقيقي والخيالي انخفضت مع زيادة نسب التطعيم حتى 7% ومن ثم عادت للزيادة مرة اخرى عند 9%. ازدادت قيم فجوة الطاقة بعد التطعيم مع NiO حيث كانت القيم في المدى 3.31 الى 3.51 eV.

Iraqi Journal of Physics by IJP is licensed under a Creative Commons Attribution 4.0 International License.

Based on a work at http://ijp.uobaghdad.edu.iq/index.php/physics.

Introduction

There have been increasing application in a wide range of fields for the use of metal oxides. It represents about a third of the consumer nanotechnology product market [1]. Metal oxides are compounds that contain at least one metal and one oxygen ion in their chemical formula such as ZnO, Fe_3O_4, TiO_2, Al_2O_3, $BaTiO_3$, and $BaZrO_3$. They play an important role in the fields of chemistry, physics, and materials science.

Nanoparticles are important as a driving force for industry and many research groups to study and understand the manufacture of these materials. The fabrication of nanoparticles can be classified into two methods "top-down" and "bottom-up", based on different physical and chemical approaches [2].

The most common semiconductor material for metal oxide is titanium dioxide (TiO_2) or titania. TiO_2 is an n-type semiconductor. It possesses three types of crystal structures consisting of rutile, anatase, and brookite phase. TiO_2 nanostructures have been used in many applications such as in photocatalysis or solar cells, lithium-ion batteries, and gas sensors. Titanium dioxide nanostructures can be fabricated by different processes, for example, anodizing, and thermal evaporation, hydrothermal and microwave-assisted. These processes can be fabricated using different nanostructures of titanium dioxide such as nanoparticles, nanotubes, and nanowires [3-5].

Doping has opened up the possibility of changing the electronic structure, the chemical composition and the optical properties of TiO_2 nanoparticles.

Much effort has gone into combining doping with metal ions, such as nickel, chromium, iron, vanadium, and zinc. Agglomerated nanoparticles, thin films, nanocomposites, nanobelts [6], Where Oja et al., attended For TiO_2 films by spray pyrolysis method at substrate temperatures from 315 to 500 °C [7]. Yingqiang et al., [8] prepared TiO_2 and fluorine doped titanium dioxide (F-TiO_2) by one-pot hydrothermal synthesis. Quartz crystal microbalance resonators (QCM) were used to detect trace levels of the stimulating nerve agent. From the dimethylphosphonate (DMMP) sensing measurements. Znad et al., Prepared photocatalysts of the mixed Ta / TiO_2- and Nb / TiO_2 oxides by simple impregnation [9]. This work deals with the preparation of doped and undoped TiO_2 thin films with various concentrations of NiO, and studying the structural and optical properties.

Experimental work

A pure semiconductor metal oxide TiO_2 mixed with an inorganic material NiO at different concentrations (3, 5, 7 and 9) wt% was prepared in this work. All TiO_2 thin films were prepared by spraying an aqueous solution of titanium (III) chloride ($TiCl_3$) from (Merck KGaA, Germany) using chemical spray pyrolysis (CPS) technique. These films were synthesized with solution molarity of (0.1M) for all experiments. The thin film TiO_2 chemical equation was formed according to [10]:

$$\begin{pmatrix} \mathbf{2TiCl_3 + H_2O \rightarrow Ti(OH)_2Cl_2 + TiCl_4} \\ \mathbf{Ti(OH)_2Cl_2 \rightarrow \downarrow TiO_2 + \uparrow 2HCl} \end{pmatrix} \qquad (\mathbf{1})$$

To prepare good quality thin films with nanostructure by chemical spray pyrolysis, different parameters such as nozzle to substrate dixtance, flow rate, solution deposition time, concentration and deposition temperature have to be considered, Fig.1. The prepared solution spray onto a substrate heated at 300 °C. The prepared thin films were annealed at 600 °C for 1 hour.

The structural and optical properties of these films were studied. XRD diffraction was done measured using X-Ray Diffractometer Shimadzu type (XRD 6000). The spectra of absorbance and transmittance were recorded in the wavelengths (300-800) nm using a computerized ultraviolet visible spectrophotometer (Shimadzu UV-1601 PC). The light sources are a halogen lamp and a deuterium socket lamp.

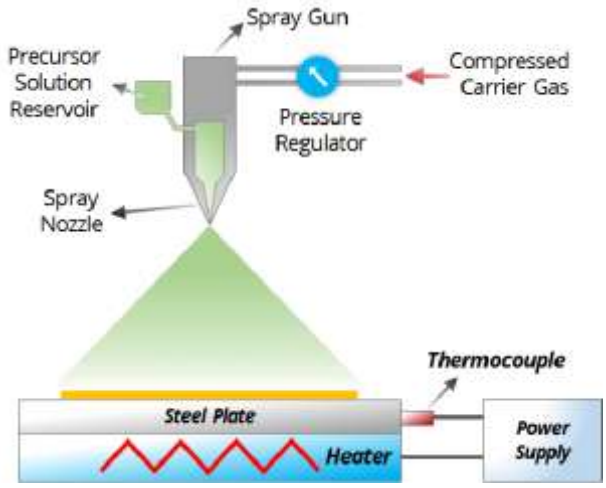


Fig.1: Schematic diagram of chemical spray pyrolysis [11].

Results and discussion

From the analysis of X-ray diffraction (XRD), the structural properties of TiO_2 and TiO_2:NiO nanostructures can be recognized over the phase of XRD studding. The XRD analysis Fig.2 of these materials showes that pure TiO_2 possesses many diffraction peaks and it hase a polycrystalline structure. This result is consistent with Yan et al., Jia et al., Al-Jawad, Panneerdoss et al. [12-15].

The crystal structure phase was found to be the anatase phase which agree with (ASTM) card no. [96-900-9087]. The (101) orientation was along the plane at diffraction angle of $2\theta = 25.2119°$, $d = 3.5169A°$ according to card no. [96-900-9087] as shown in Table 1.

After doping with NiO in different concentrations (3, 5, 7, and 9) %, the peaks showed variation in their intensities. The peaks intensity decreased after doping until the structure converted from polycrystalline to amorphous up to 7% and hence the intensity of peaks returned increased again at 9% percentage. There was an increase in full width of half maximum FWHM to more peaks but decreased of crystallite size with increased doping percentage.

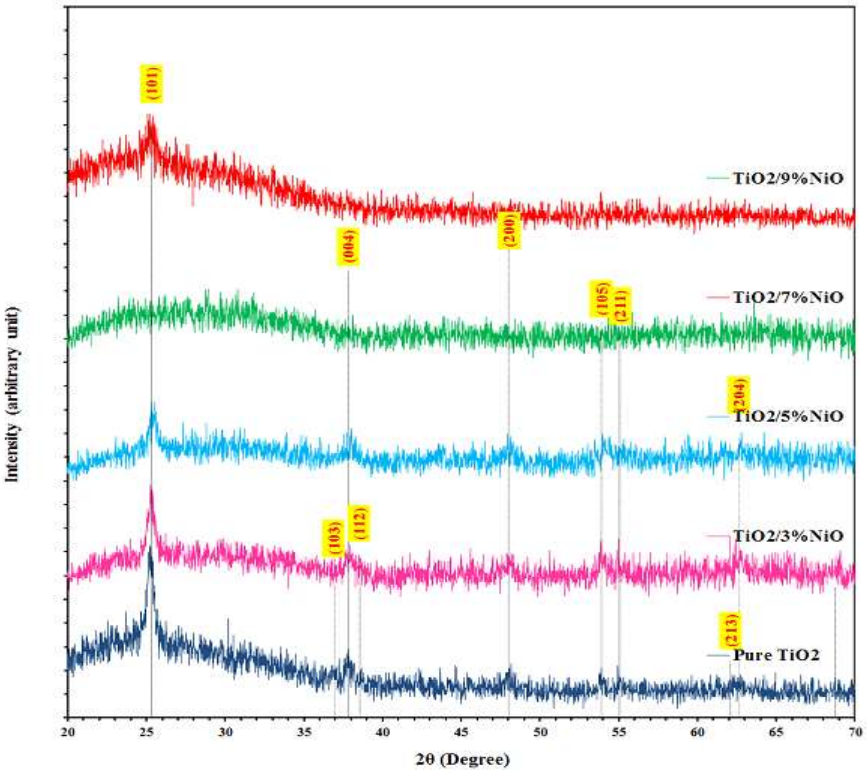


Fig.2: XRD of TiO_2 doped and undoped thin films.

Table 1: The structure properties of TiO_2 samples.

NiO%	2θ (Deg.)	FWHM (Deg.)	d_{hkl} Exp.(Å)	G.S (nm)	d_{hkl} Std.(Å)	Phase	hkl	card No.
0	25.2119	0.5728	3.529526	14.21181	3.5169	Anatase	(101)	96-900-9087
	37.8121	0.6873	2.377342	12.21783	2.3785	Anatase	(004)	96-900-9087
	48.0069	0.7446	1.893598	11.67921	1.8925	Anatase	(200)	96-900-9087
	53.8488	0.63	1.701138	14.14302	1.7001	Anatase	(105)	96-900-9087
	54.937	0.3436	1.669988	26.05846	1.6665	Anatase	(211)	96-900-9087
	62.6811	0.5330	1.480994	17.45114	1.4809	Anatase	(204)	96-900-9087
3	25.2692	0.5727	3.521652	14.21588	3.5169	Anatase	(101)	96-900-9087
	37.9267	0.8019	2.370422	10.47537	2.3785	Anatase	(004)	96-900-9087
	48.0641	0.6873	1.891478	12.65572	1.8925	Anatase	(200)	96-900-9087
	53.9061	0.7446	1.699465	11.96933	1.7001	Anatase	(105)	96-900-9087
	54.937	0.5727	1.669988	15.63417	1.6665	Anatase	(211)	96-900-9087
	62.7262	0.8019	1.480037	11.60205	1.4809	Anatase	(204)	96-900-9087
5	25.3837	0.63	3.506026	12.92581	3.5169	Anatase	(101)	96-900-9087
	37.984	0.8019	2.366977	10.47717	2.3785	Anatase	(004)	96-900-9087
	48.0641	0.8018	1.891478	10.84843	1.8925	Anatase	(200)	96-900-9087
	53.9633	0.6873	1.697799	12.97051	1.7001	Anatase	(105)	96-900-9087
	62.7835	0.5154	1.478824	18.0569	1.4809	Anatase	(204)	96-900-9087
7				Amorphous				
9	25.2692	0.8018	3.521652	10.15395	3.5169	Anatase	(101)	96-900-9087

The UV-Vis transmission spectrum in the (300-800) nm region is shown in Fig.3 for TiO_2 and TiO_2:NiO films. The figure shows that the intensity of transmittance increases with increasing wavelength and with increasing concentration of NiO. The increase of concentration of NiO resulted in reduction of crysttallite size which in turn shift the energy gap to the high energy side. The crystal size decreased from 14.21 to 12.92 nm as the doping ratio increased from 0 to 5%. The transmittance increased

with increasing of doping ratio for law doping ratio but it decreased at the 9%. This decrease causes a decrease in absorption within the visible region of the spectrum. The transmittance increases and is nearly constant at (44, 49, 57, 62 and 61) % for the concentrations (pure, 3, 5, 7 and 9) % respectively at wavelength 500nm, Table 2. These results of transmittance are in agreement with those of Essalhi et al. [16].

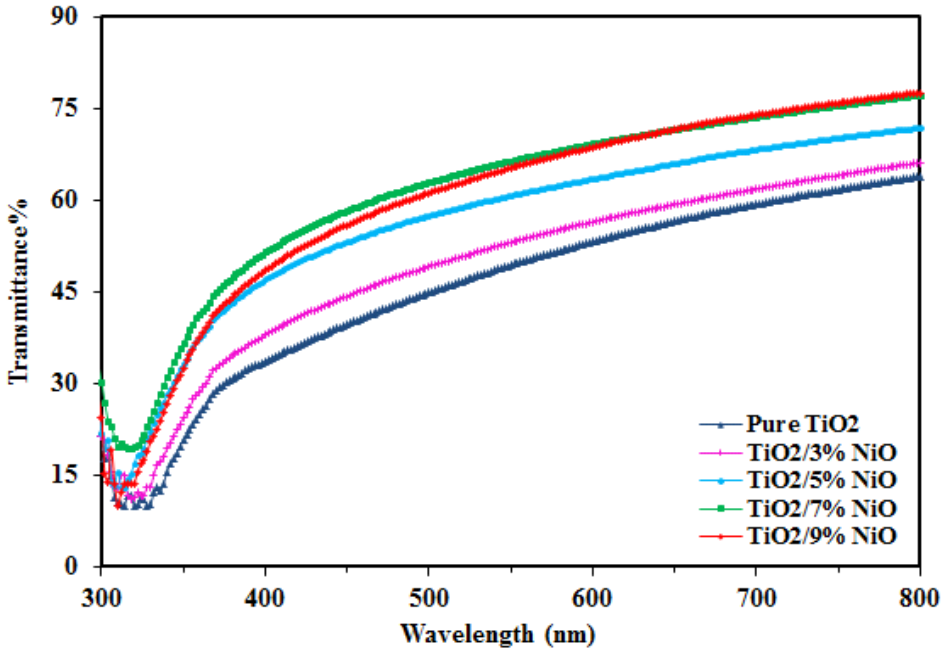


Fig.3: Transmission spectra of TiO_2 doped and undoped thin films.

Optical band gap values were estimated according to Tauc's equation Eq. (2):

$$\alpha h\nu = B'(h\nu - E_g)^{1/2} \qquad (2)$$

where B' is inversely proportional to amorphouscity, ν is the optical frequency. To calculate the band gap energies of pure TiO_2 and of those doped with NiO thin films. $(\alpha h\nu)^2$ was drawn as a function of the incident radiation energy as shown in Fig.4. A typical optical energy gap was determined at the highest absorption region where $\alpha > 10^4\ cm^{-1}$ plotted $(\alpha h\nu)^{1/r} = 0$ where r = 1/2 for direct allowed transition [17].

From Fig.4 it can be observed that direct optical band gap energy for pure TiO_2 films is 3.31 eV, this result agrees with that of Cetin et al. Scanlon et al. Prasai et al. Rojviroon et al. [18-21]. The optical energy gap increased with the increase of doping ratio of NiO, It increased from 3.31eV to 3.51eV with the increase of doping up to 7% after that decrease in the value of the energy gap to 3.49 eV was noticed at 9% doping, Table 2. This shift towards the higher energy of the optical energy gap is associated with a reduction in the size of the crystals responsible for reducing the absorption coefficient [22-23].

Table 2: The optical properties of TiO_2 samples at 500 nm.

NiO%	T%	E_g(eV)	n	k	ε_r	ε_i
0	44.86	3.31	2.590	0.340	6.592	1.762
3	49. 08	3.40	2.577	0.302	6.552	1.557
5	57.52	3.45	2.480	0.235	6.098	1.165
7	62.92	3.51	2.380	0.196	5.628	0.936
9	61.12	3.49	2.410	0.209	5.796	1.01

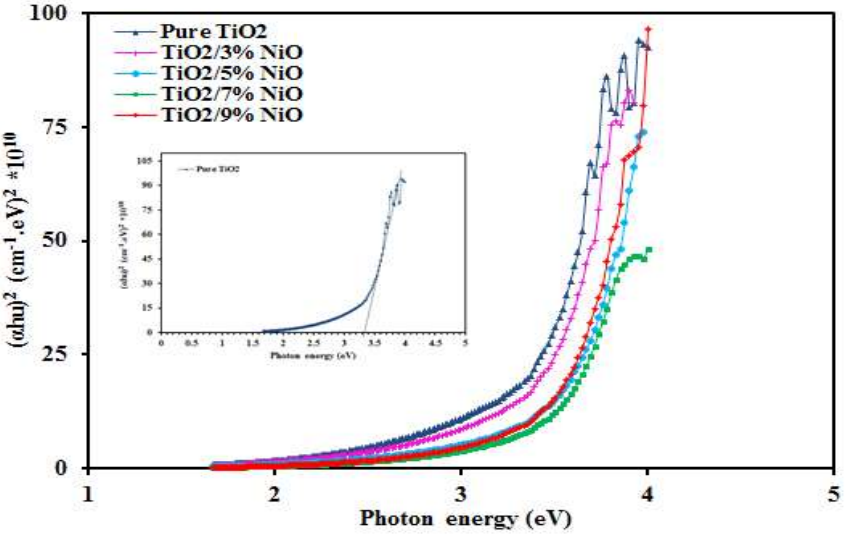


Fig.4: Variation the $(\alpha h\nu)^{1/2}$ as a function of photon energy.

An important parameter for optical materials and applications is the refractive index (n). The refractive index of all films was determined from the relationship [24]:

$$n = \left(\frac{1+R}{1-R}\right) + \sqrt{\frac{4R}{(1-R)^2} - K^2} \qquad \textbf{(3)}$$

where R is reflectance, k is extinction coefficient. The variation of refractive index of the TiO_2 and TiO_2:NiO samples for different doping percentage with wavelength of the incident photon is shown in Fig.5. High refractive index is observed in the short wavelengths followed by a gradual decrease in the high wavelength.

The refractive index of TiO_2 films was found to increase after continuous addition of NiO at short wavelengths then decreased at long wavelengths up to 7% and increased again at 9% doping. The calculated experimental values were (2.59, 2.57, 2.48, 2.38 and 2.41) for samples (pure, 3, 5, 7 and 9) % respectively at 500 nm. The increase of refractive index is attributed to the reduction of transmittance giving rise to high opaque material. The refractive index values obtained agree with the results reported by Sta et al. [25].

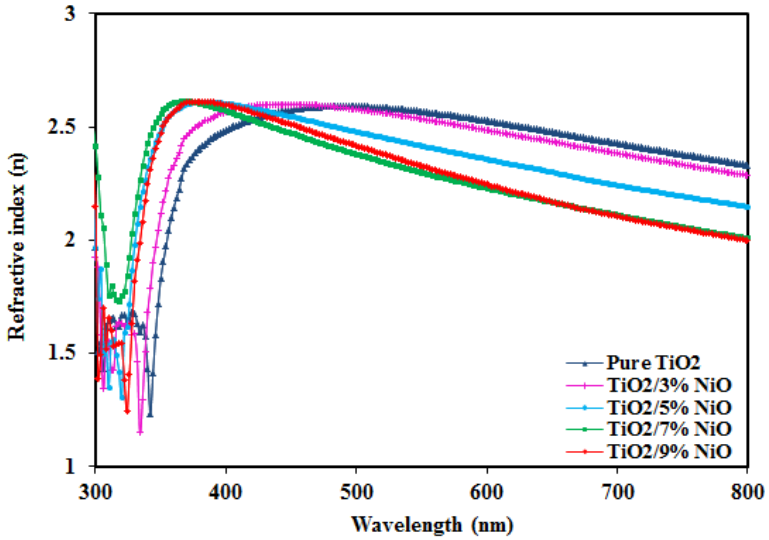


Fig.5: The variation of refractive index with wavelength for pure and doped TiO_2 films.

Fig.6 shows the dependence of the extinction coefficient (k) on the wavelength in the range (300-800) nm for undoped and doped samples. The figure show that the extinction coefficient for pure TiO_2 sample showed a decrease in the wavelengths range (330-800) nm and with after doping the samples (3, 5, 7 and 9) %, in theses wavelengths. Extinction coefficient showed continuous decrease for doping concentrations (3, 5 and 7) % and after that increased again for 9%.

The decrease and increase of the extinction coefficient associated with a decrease and increase in the absorption coefficient accompanied the addition of impurity atoms. The extinction coefficient is calculated by the below equation [26]:

$$k = \frac{\alpha\lambda}{4\pi} \qquad (4)$$

where α is the absorption coefficient.

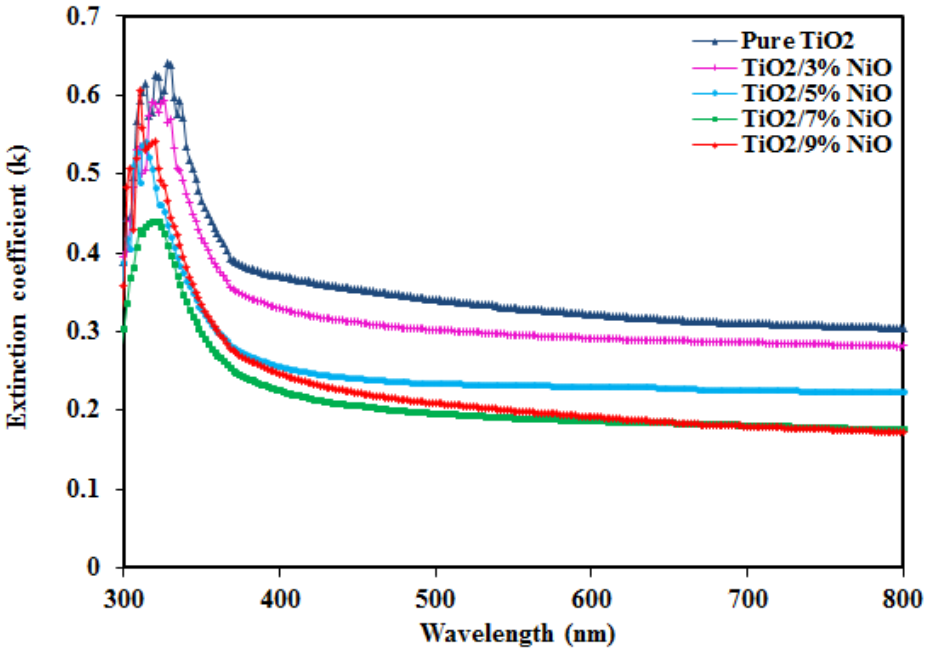


Fig.6: The Extinction coefficient versus wavelength for undoped and doped TiO_2 thin films.

The real dielectric constant is ε_r and the imaginary parts ε_i are related to the values of (n) and (k). Real and imaginary values were calculated by using equations [27]:

$$\varepsilon_r = n^2 - k^2 \qquad (5)$$

$$\varepsilon_i = 2nk \qquad (6)$$

Dependence of the real part on wavelength is shown in Fig.7 for the pure and doped thin films. Real part values show suggestion increase in the short wavelengths at (320-370) nm of all films and then slightly decreased was happened in the wavelength range (370-800) nm. On the other hand, in the high wavelength curves of real part was decreased with increasing concentration up to 7% and then there was an increase again at 9%. The measured values at wavelength 500nm were (6.592, 6.552, 6.098, 5.628 and 5.796) for samples (pure, 3, 5, 7 and 9) % as shown in Table 2.

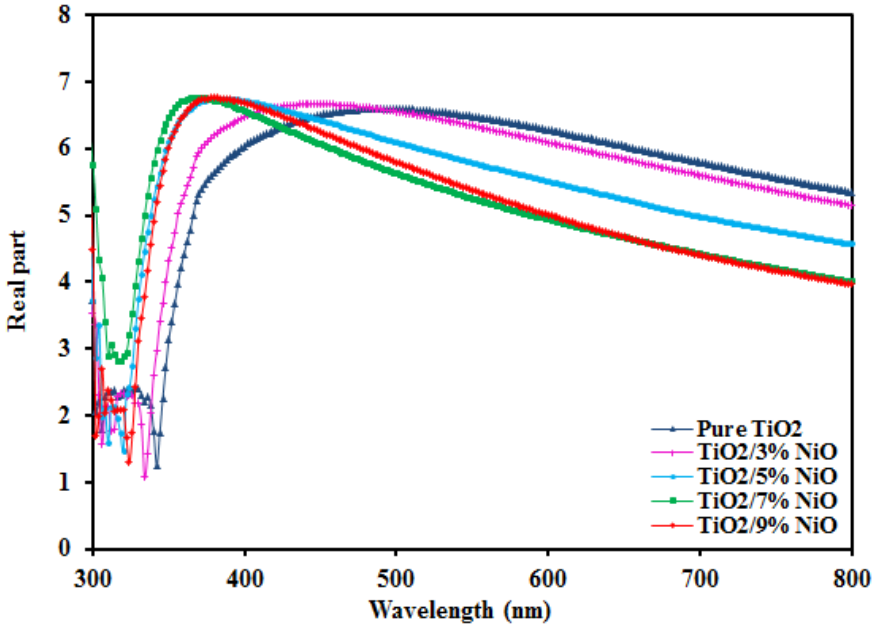


Fig.7: The variation is the real part of the dielectric constant as a function of the wavelength of the pure and doped TiO_2 thin films.

Fig.8 shows the imaginary part of dielectric constant as a function of wavelength in range (300-800) nm. The figure clearly showed the dependence of the imaginary part on the extinction coefficient Eq.(6) because it is very small refractive index [28, 29].

The imaginary part decreased, as NiO was added to the host material in different concentrations up to 7% and then increased with more addition of NiO. The measured values, at wavelength 500nm were (1.762, 1.557, 1.165, 0.936 and 1.01) for samples (pure, 3, 5, 7 and 9) % as show in Table 2. The same reason previously mentioned to k can be given here to explain the behavior of ε_i.

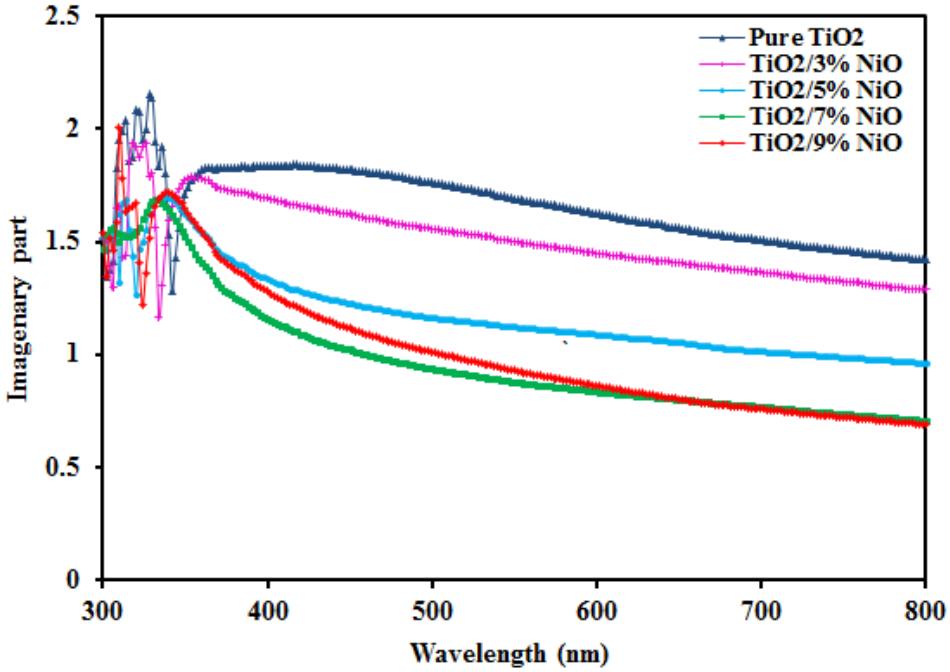


Fig.8: The imaginary part of dielectric constant versus wavelength for undoped and doped TiO_2 thin films.

Conclusions

The results indicate that nanosize of pure and doped TiO_2 with Nickle oxide NiO can be achieved which can affect the structure and optical properties. XRD analysis showed that all the prepared thin films from pure TiO_2 and doped with Nickle oxide up 5% have polycrystalline structure with anatase phase. Increases of doping ratio up to 7% reduced the crystallte size till change the structure from crystalline to amorphous and shift the energy gap to higher energies and then polycrystalline structure return to appear with further increase of doping ratio and the energy gap reduced to slightly. The refractive index and real part dielectric constant increased while extinction coefficient and imaginary dielectric constant reduced by addition of NiO to TiO_2 up 7% and then the inverse manner took place.

Acknowledgment

The authors acknowledge the Al- Nahrain University, College of science, Department of Physics and Baghdad University, Department of Physics.

References

[1] A. D. Maynard, R. J. Aitken, T. Butz, V. Colvin, K. Donaldson, G. Oberdörster, Nature, 444 (2006) 267-9.
[2] P. Grundler. Chemical sensors: An intro-duction for scientist and engineers: Springer, Berlin Heidelberg. (2007).
[3] R. Kumara, N. Sharmab, N. Arora: Advances in Applied Science Research, 7, 3 (2016) 142-147.
[4] Ch. Girginov, P. Stefchev, P. Vitanov, Hr. Dikov, Journal of Engineering Science and Technology, 5, 4 (2012) 14-17.
[5] J. I. Arishi and J. Ozuomba, Chemical Science International Journal, 24, 4 (2018) 1-10.
[6] S. B. Eadi, S. Kim, S. W. Jeong, H. W. Jeon, Hindawi, Advances in Materials Science and Engineering, 2017 (2017) 1-6.
[7] I. Oja, A. Mere, M. krunks, Solid State Phenomena, 99-100 (2004) 259-264.
[8] Z. b Yingqiang, D. b. Xin, W. Xiaoying, H. Junhui, Y. Yunbo, H. Hong, Sensors and Actuators B. 151 (2010) 205-211.
[9] Z. Hussein, H.A. Ming, O.T. Moses: Hindawi, International Journal of Photoen-ergy, 2012 (2012) 1-9.
[10] A. A. Hateef, B. D. Balawa, A. F. Saleh, M. W.Mahmmod, International Research Journal of Engineering Science, Technology and Innovation (IRJESTI). 1, 6 (2012) 175-179.
[11] S.I. Park, Y.J. Quan, S. H Kim, H. Kim, S. Kim, D. M. Chun, C. S. Lee, M. Taya, W. S. Chu, S. H. Ahn: International Journal of Precision Engineering and Manufacturing-Green Technology, 3, 4 (2016) 397-421.
[12] W. Y. Yan, Q. Zhou, X. Chen, X. J. Huang, Y. C. Wu, Sensors and Actuators B: Chemical, 230 (2016) 761-772.
[13] Y.J. Jia, W.X. Su, Y.B. Hu, H.N. Chen, Bulgarian Chemical Communications. 49 (2017) 190-192.
[14] S.M.H. Al-Jawad, International Journal of Scientific & Engineering Research, 5, 1 (2014) 2171-2176.
[15] I. J. Panneerdoss, S.J. Jeyakumar, M. Jothibas: Research Inventy, International Journal Of Engineering And Science, 4, 11 (2014) 15-20.
[16] Z. Essalhi, B. Hartiti, A. Lfakir, M. Siadat, P. Thevenin,: J. Mater. Environ. Sci. 7, 4 (2016) 1328-1333.

[17] W. A. Al-Taa'y, M. T. Abdul nabi, T. K.Al-Rawi, Baghdad Science Journal, 8, 2 (2011) 543-550.
[18] S.S. Cetin, S. Corekci, M.Cakmak, S. Ozcelik: Cryst. Res. Technol, 46, 11 (2011) 1207-1214.
[19]D.O. Scanlon, C.W. Dunnill, J. Buckeridge, S.A. Shevlin, A.J. Logsdail, S.M. Wo odley, C.R.A. Catlow, M.J. Powell, R.G. Palgrave, I.P. Parkin, G.W. Watson, T.W. K eal, P. Sherwood, A. Walsh, A. A. Sokol: Nat. Mater, 12, 9 (2013) 798-–801.
[20]B. Prasai, B. Cai, M. K. Underwood, J. P. Lewis and D.A. Drabold, J. Mater. Sci., 47, 21 (2012) 7515-7521.
[21] T. Rojviroon and S. Sirivithayapakorn, Surf. Eng., 29, 1 (2013) 77-80.
[22] D.U. Onah, A.B.C Ekwealor, B.A. Ezekoye, R.U. Osuji, F.I Ezema, C.E.Okeke, Journal of Ovonic Research, 8, 5 (2012) 105-111.
[23] M. Bhendea, R. Bobadea, S. Yawaleb, S.Yawale: Sci. Revs. Chem., 2 (2012) 413-418.
[24] W.A. Al-Taa'y, S. F. Oboudi, E. Yousif, M. Abdul Nabi, R. M. Yusop, D.Derawi: Hindawi Publishing Corporation, Advances in Materials Science and Engineering, 2015 (2015) 1-5.
[25] I.Sta, M.Jlassi, M.Hajji, M.F. Boujmil, R. Jerbi, M.Kandyla, M. Kompitsas, H.Ezzaouia, Science and Technology, 72 (2014) 421-427.
[26] Y.Al-Ramadin, Optical Material, 14 (2000) 287-290.
[27] E.I. Ezema, P.U. Asogwa, P.E. Ekwea-lor, P.E. Ugwuoke, R.U. Osuji, Journal of the University of Chemical Technology and Metallurgy, 42 (2007) 217-222.
[28] K.A. Khadum, Diala Journal, 32 (2009) 1-15.
[29] A.H. Ahmad, A.M. Awatif, N. Z. Abdul-Majied, Eng & Technology, 25 (2007) 558-568.